EP53E-2289 - Inverse Modeling of Turbidity Currents using 2D Shallow-Water Model and Neural Network toward understanding of development processes of submarine fans

Hajime NARUSE (Kyoto University)

sponsored by
Sediment Dynamics Research Consortium
INPEX JAPEX
JOGMEC
JX Nippon Oil & Gas Exploration Corporation

1. Introduction

Aim

Establish an inversion method to "measure" flow conditions from ancient turbidites

Backgrounds

In-situ measurements of turbidity currents revealed that they exhibit monthly to yearly recurrence intervals. However, ancient turbidites generally exhibit sub-millenial scale of recurrence interval. Are they different type of flows? What is the dominant fan-building process?

To answer this question, we need to measure flow conditions from geologic records.

Difficulty

Inversion of turbidity currrents are difficult subject for inversion because of their non-linear behavior. Most of previous attempts optimized their forward model parameters to reporoduce the specific ancient deposits, which successed little.

Solution

This study established the inverse model by the artificial neural network (NN), which is trained by the forward model. This model seeks general relationship between product and causes.

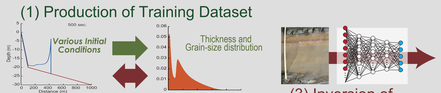

Fig. 1. Concept of the inversion by the neural network. Numerical simulation was repeated to obtain horizontal distribution of thickness of turbidites under various initial conditions, and then this synthetic data set was used for supervised training of DNN. After the training phase finished, DNN properly estimated initial conditions of turbidity currents (e.g. initial flow height, velocity, etc.) from artificial test data set that was also produced from the forward model.

Neural Network Learns Cause/Products from Forward Model

2. Forward Model: 2D Shallow Water Model

Model Formulation

$$\frac{\partial h}{\partial t} + U\frac{\partial h}{\partial x} + V\frac{\partial h}{\partial y} = e_w\sqrt{U^2+V^2} - h\left(\frac{\partial U}{\partial x} + \frac{\partial V}{\partial y}\right) \quad (1)$$

$$\frac{\partial U}{\partial t} + U\frac{\partial U}{\partial x} + V\frac{\partial U}{\partial y} = -Rg\tilde{C}\frac{\partial \eta}{\partial x} - \frac{1}{2}Rgh\frac{\partial \tilde{C}}{\partial x} - Rg\tilde{C}\frac{\partial h}{\partial x} - \frac{u_*^2}{h} - \frac{e_w U\sqrt{U^2+V^2}}{h} + \nu_t\left(\frac{\partial^2 U}{\partial x^2} + \frac{\partial^2 V}{\partial y^2}\right) \quad (2)$$

$$\frac{\partial V}{\partial t} + U\frac{\partial V}{\partial x} + V\frac{\partial V}{\partial y} = -Rg\tilde{C}\frac{\partial \eta}{\partial y} - \frac{1}{2}Rgh\frac{\partial \tilde{C}}{\partial y} - Rg\tilde{C}\frac{\partial h}{\partial y} - \frac{v_*^2}{h} - \frac{e_w V\sqrt{U^2+V^2}}{h} + \nu_t\left(\frac{\partial^2 U}{\partial x^2} + \frac{\partial^2 V}{\partial y^2}\right) \quad (3)$$

$$\frac{\partial C}{\partial t} + U\frac{\partial C}{\partial x} + V\frac{\partial C}{\partial y} = \frac{w_s(e_s - r_0 C)}{h} - \frac{e_w C\sqrt{U^2+V^2}}{h} \quad (4)$$

$$\frac{d\eta}{dt} = \frac{w_s(r_0 C - e_s)}{1-\lambda_p} \quad (5)$$

where U, V are layer-averaged horizontal velocity components. C is a sediment concentration, and h denotes flow height. R is submerged specific density of sediment particles, and w_s is settling velocity. u_* and v_* are shear velocities. The parameter ν_t denotes eddy viscosity ($=1/6\alpha u_* h$). Momentum equation (2) and (3) are solved by Il-CIP-M Method (3rd order accuracy). Mass conservation equations of fluid (1) and sediment (2) are solved by implicit scheme. Artificial viscosity is added for numerical stability on the basis of Jameson (1981). Dry/wet boundary grids are solved using the scheme proposed by Yang et al. (2016). Entrainment coefficients e_s and e_w are calculated using Garcia and Parker (1991) and Parker (1987).

Implemented by Python and Cython with numpy and landlab. Code available at GitHub (https://github.com/narusehajime/turb2d.git)

Turb2d: Horizontal 2D Model of Turbidity Currents

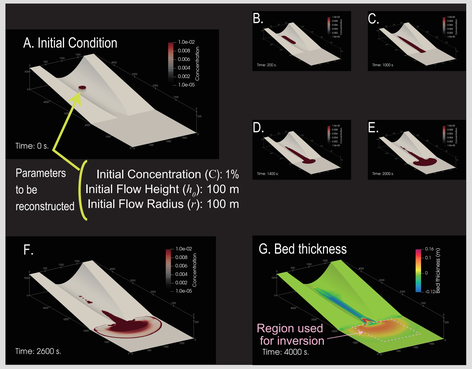

Fig. 2. Example of simulation of turbidity currents. Visualization of results was done by the software paraview. Turbidity current initiates from the lock-exchange condition, and flows down to the basin plain. A-F: time development of flow height and concentration. G: Final thickness distribution of the bed.

3. 2D CNN Inverse Model

Convolutional Neural Network connected with Fully Connected Layers

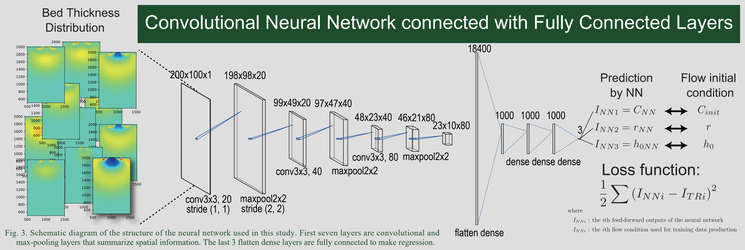

Fig. 3. Schematic diagram of the structure of the neural network used in this study. First seven layers are convolutional and max-pooling layers that summarize spatial information. The last 3 flatten dense layers are fully connected to make regression.

Over 300 simulation runs produced pairs of bed thickness and flow initial conditions that were determined randomely. This was done by PC and supercomputing service at Kyoto University. Then, supervised training of NN was conducted. Convolutional neural network summarise topographic features, and regression to the initial conditions was performed by dense layers.

Neural Network discovers empirical relationship between bed/flow condition by supervised training

Environment and Calculation Settings	
Libraries	Python3.6.8, Keras2.2.4, TensorFlow-GPU1.15.0, CUDA10.0, CuDNN7.6
CPU and GPU	Intel Core I 7 8700k & GTX1080Ti
Optimization method	SGD (learning rate = 5.0×10^{-3}) with momentum 0.9
Batch size	32
Number of epochs	1000
Number of Training Data	500
Validation split	10% of training data

4. Training and Verification

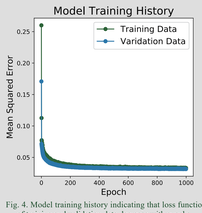

Fig. 4. Model training history indicating that loss function of training and validation data decrease with epochs.

Trained NN can predict unknown test conditions adequately from deposits

History of model training describes that the training was successfull and overfitting to training set did not occur. Loss function decreased rapidly and show no large discrepancy between those of training and validation sets.

Using test dataset that are indipendent from dataset used in the training phase, the model reasonably estimated the flow initial condition and height, whereas initial radius show large scatter.

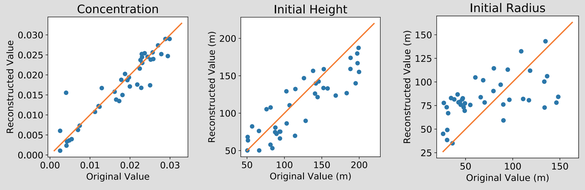

Fig. 5. Scatter diagrams exhibiting precision and accuracy of the inverse model. Orange line is 1:1 line that indicates perfect reconstruction of original flow parameters. Initial sediment concentration was well reconstructe, and initial height is reasonably estimated.

5. Results from Incomplete Data

A. Dataset with noise

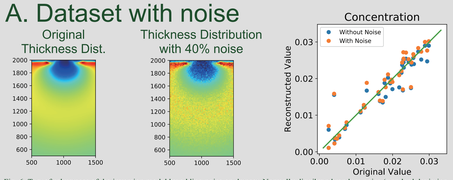

Fig. 6. Test of robustness of the inversion model by adding noise on dataset. Normally distributed random noise (standard deviation is 40 % of original thickness) was added on the thickness distribution. Comparison between two inversion using from original and data with noise indicates that random noise has almost no influence on results.

B. Subsampled data

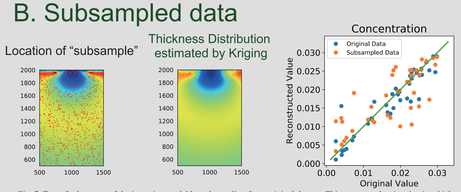

Fig. 7. Test of robustness of the inversion model by subsampling from original dataset. This supposes the situation in which thickness data are only available at limited locations such as places where well-logs were taken. Thickness data at 5% of original grids were subsampled, and the entire distribution was estimated by ordinary Kriging. Then, interpolated data were analyzed by the inverse model. As a result, even though results from subsampled data scattered largely comparing the original result, they still keep reasonable precision.

The inverse model is robust against incomplete dataset

Two tests were conducted to verify robustness of the inversion model.

First, normally distributed randome noise was added on input thickness. Measurements are always accompanied with errors. The inverse model analyzed the dataset with artificial noise, but almost no influence was observed in inversion result.

Secondly, thickness distribution in the test dataset was subsampled to 5%. In natural conditions, it is rare that the entire thickness distribution of a turbidite is available, so that distribution is necessary to be estimated from limited data. Here the inversion was conducted on dataset where the bed geometry was estimated from subsampled data by ordinary Kriging. Again, inversion result was less affected by this interpolation process.

These results imply that the inversion model using NN is robust against the incomplete datasets, and thus it can be expected to be applied for natural complex phenomena.

6. What's next?

Inversion of two dimensional turbidity currents is now possible by deep-learning neural network

The model is robust and can be applied to deposits developed on complicated topography

The millenial scale event, 2011 Tohoku-Oki Tsunami-generated turbidity current is possible target for future application.

Numerical simulation and core sample of Tsunami-generated turbidity current

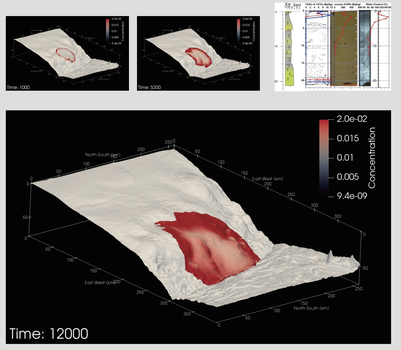

Fig. 8. An example of numerical simulation of a turbidity current around Japan Trench. It has been indicated that 2011 Tohoku-Oki Tsunami generated a very large-scale turbidity current along NE Japan and Japan Trench (Arai et al., 2013). Modern turbidites were discovered from cores taken after the event. The recurrence interval of this tsunami event is ~1000 years, and the seismogenic turbidites are expected to be clues for magnitude of past events. IODP cruise to take the sample is planned next year.

References

Arai, K., Naruse, H., Miura, R., Kawamura, K., Hino, R., Ito, Y., ... & Kasaya, T. (2013). Tsunami-generated turbidity current of the 2011 Tohoku-Oki earthquake. Geology, 41(11), 1195-1198.
Garcia, M., & Parker, G. (1991). Entrainment of bed sediment into suspension. Journal of Hydraulic Engineering, 117(4), 414-435.
Jameson, A., Schmidt, W., & Turkel, E. (1981, June). Numerical solution of the Euler equations by finite volume methods using Runge Kutta time stepping schemes. In 14th fluid and plasma dynamics conference (p. 1259).
Parker, G., Garcia, M., Fukushima, Y., & Yu, W. (1987). Experiments on turbidity currents over an erodible bed. Journal of Hydraulic Research, 25(1), 123-147.
Yang, H., et al., 2016, A study on the water front in shallow water equations. Japan Civil Engineering